International Journal of Environmental Science and Technology (2021) 18:163–172
https://doi.org/10.1007/s13762-020-02842-6

ORIGINAL PAPER

Investigation of mechanism and kinetics in the TiO_2 photocatalytic degradation of Indigo Carmine dye using radical scavengers

J. S. G. Neto[1] · S. Satyro[2] · E. M. Saggioro[3] · M. Dezotti[1]

Received: 26 February 2020 / Revised: 5 June 2020 / Accepted: 6 July 2020 / Published online: 13 July 2020

Abstract

This study is aimed at investigating the influence of different scavenger species of radicals that might possibly be involved in the TiO_2/UVA photocatalytic degradation of Indigo Carmine dye. The effect caused by the presence of hydroxyl radicals (1-butanol and 2-propanol), positive holes (h^+) (potassium iodide) and singlet oxygen (azide) was studied. Kinetics and optimal degradation conditions were evaluated using a factorial experiment design. The highest pseudo-first-order kinetics ($k = 5.22 \times 10^{-2} \pm 0.002$ and $t_{1/2} = 13.25 \pm 0.49$ min) was achieved at pH 4.0, 6 mg L^{-1} of Indigo Carmine dye and 12 mg L^{-1} of TiO_2. Mineralization was not achieved, and direct photolysis was not observed under the studied conditions. Indigo Carmine degradation occurs mainly due to oxidation in the positive hole (h^+) followed by singlet oxygen action and on a smaller scale by hydroxyl radical. The use of the aforementioned radical scavengers made it possible to verify the mechanism and kinetics of Indigo Carmine dye through TiO_2 heterogeneous photocatalysis.

Keywords Heterogeneous photocatalysis · Advanced oxidative processes · Factorial experiment design · Wastewater treatment

Introduction

The increase in the complexity of wastewater composition, along with government impositions regarding the improvement in effluent quality, has promoted the search for new methodologies for wastewater treatment (Cerreta et al. 2020). In general, waste produced by industrial activities contains toxic pollutants that are resistant to conventional treatment systems, such as coagulation/flocculation, activated carbon adsorption, precipitation and biological degradation. It is necessary to develop methods able to break down hazardous organic compounds present in wastewaters (Zulmajdi et al. 2020). Currently, different methods involving the elimination or conversion into smaller, less toxic or inert molecules are available for minimizing the impact of wastewater discharge into water bodies (Kumar et al. 2020). Hydroxyl radicals ($^{\cdot}OH$) display one of the highest oxidation potentials, and they are often used in these methods. These radicals are non-selective and can promote the degradation of several compounds through a fast reaction. Many ways to produce hydroxyl radicals have been studied, frequently using ozone, hydrogen peroxide, semiconductors (i.e., TiO_2) or the Fenton reagent (Brillas 2020).

In general, when semiconductors are irradiated, electrons (e^-) migrate from the valence band to the conduction band, leaving a positive hole (h^+) in the valence band. Therefore, the holes can produce hydroxyl radicals by oxidizing both water and hydroxyl groups (Jiménez et al. 2015). On the other hand, conduction band electrons easily react with molecular oxygen leading to the formation of superoxide radical anions ($O_2^{\cdot-}$) and/or hydroperoxide radicals ($HO_2^{\cdot}$),

Editorial responsibility: Parveen Fatemeh Rupani.

Electronic supplementary material The online version of this article (https://doi.org/10.1007/s13762-020-02842-6) contains supplementary material, which is available to authorized users.

✉ E. M. Saggioro
saggi_br@hotmail.com

[1] COPPE - Chemical Engineering Program, Federal University of Rio de Janeiro, Rua Horácio Macedo 2030, Cidade Universitária, Rio de Janeiro, RJ 21941-450, Brazil

[2] Department of Chemical and Biological Engineering, The University of British Columbia, 2360 E Mall, Vancouver, BC V6T 1Z3, Canada

[3] Sanitation and Environmental Health Department, Sergio Arouca National School of Public Health, Oswaldo Cruz Foundation, Av. Leopoldo Bulhões 1480, Rio de Janeiro, RJ 21041-210, Brazil

which promotes the formation of hydroxyl radicals (Rodríguez-González et al. 2020).

The degradation pathway using Indigo Carmine (IC) dye as a model of the persistent organic pollutants group has been studied using different photocatalysts. For instance, IC dye was degraded by h^+ and $O_2^{\cdot-}$ when Ag_2SO_4/ZnO ($10\%_{wt}$) was used as the photocatalyst (Choo et al. 2016), and by superoxide radical ($O_2^{\cdot-}$) when BiOBr-Ag_8SnS_6, an heterostructured nanocomposite (Chowdhury and Shambharkar 2018), zirconium oxide nanocomposite (GO–ZrO_2) (Das et al. 2019) and nanostructured CdS semiconductors (Hernández-Gordillo et al. 2016) were tested as the photocatalysts. Nonetheless, when α-Bi_2O_3/C-dots was tested, $^{\cdot}OH$ radical and electrons (e^-) were the primary and main reactive species (Sharma et al. 2019). Finally, $^{\cdot}OH$ radical was also found as the main reactive species when a Mg/ZnO-GO composite (Labhane et al. 2018) and a mesoporous Nb_2O_5 nanomaterial (Silva et al. 2020) were tested.

Heterogeneous photocatalysis using titanium dioxide (TiO_2) and UV light is among the most studied advanced oxidative processes (AOP) in the recent years, playing an important role concerning the latest water treatment technologies (Rodríguez-González et al. 2020). The non-selectivity of the produced hydroxyl radicals is one of the reasons for the application of AOP on the treatment of wastewater. This non-selectivity was explored on the very early stages of the development of AOP (Höfl et al. 1997). There are many advantages on the use of TiO_2 in water treatment, such as easy handling, low cost, high photochemical reactivity and stability in a wide pH range (Rodríguez et al. 2014). Even though TiO_2/UV heterogeneous photocatalysis has been largely studied, only one study was found involving reactive species on the IC dye degradation using TiO_2 (Bi–Zn co-doped TiO_2). In this particular case, it was observed a decrease on the order of participation of the reactive species ($h^+ > O_2^{\cdot-} > {}^{\cdot}OH$) (Benalioua et al. 2015).

Different studies have been done in order to understand the degradation pathways of various organic compounds in order to assist on achieving higher oxidation rates (Jiménez et al. 2015; Bosio et al. 2018). Moreover, the effect of scavengers present on the wastewater as a result of its diversity has been also reported. Rodríguez et al. (2014) observed that the wastewater composition may affect the degradation pathway of organic compounds. As aforementioned, the mechanisms of IC dye degradation can occur via several pathways (positive holes, singlet oxygen action, hydroxyl and superoxide anion radicals). However, the mechanism of IC dye degradation is not completely clarified when TiO_2(P25)/UV photocatalysis is applied. Therefore, in order to efficiently increase the reaction rate of this process, it is needed a better understanding of the pathway of photoreactive species involved in the IC dye degradation. The conditions in which such investigation is carried out might interfere on how accurate the results are, requiring a prior optimization of these conditions. Therefore, it is important to determinate the range in which important factors, such as pH, temperature and ionic strength, lead to the best possible response. Thus, it would be necessary to perform several experimental runs at fixed conditions to evaluate each factor, One Factor At a Time (ODAT). However, a good strategy of experimentation can limit the number of experiments performed, leading to a noticeable reduction in performance-related costs, while experiments still achieve a high level of confidence under standardized tests. One of the possible approaches is to vary the factors together instead of one at a time, a factorial experiment (Salehi et al. 2017).

In this context, this study evaluated optimal degradation conditions of the Indigo Carmine (IC) dye by heterogeneous photocatalytic using TiO_2/UV. The IC dye was the chosen organic compound due to side effects caused in wildlife if dyes are disposed into the environment. Such effects include permanent injury to cornea and different disorders, such as reproductive, developmental and neuronal (Saggioro et al. 2015b, a). Moreover, IC degradation has been thoroughly evaluated, but little is known about its oxidation pathway using TiO_2 heterogeneous photocatalysis. That said, this study brings for the first time the investigation of IC dye degradation pathway at optimum conditions using positive hole (h^+), hydroxyl radical ($^{\cdot}OH$) and singlet oxygen ($^1O_2$) scavengers.

Materials and methods

Materials

The photocatalyst used was the commercial titanium dioxide AEROXIDE® TiO_2 P25 (Evonik). Sodium hydroxide (0.1 M NaOH) and hydrochloric acid (0.1 M HCl) were used for pH adjustments. Sodium bicarbonate ($NaHCO_3$) was supplied by Isofar, Indigo Carmine dye (85%) and sulfuric acid (H_2SO_4) by Sigma-Aldrich Brazil. Nessler reagent (potassium tetraiodomercurate (II) alkaline solution), used to determine free ammonia, was prepared following Rand et al. (1974) using mercury iodide (HgI_2) supplied by Sigma-Aldrich. Iso-propyl alcohol P.A. (2-propanol), normal butyl alcohol P.A. (1-butanol) and sodium azide (Na_3N) supplied by Vetec, tert-butanol supplied by Tedia Brazil and potassium iodide P.A. (KI) supplied by Synth were used on the investigation of the photocatalytic degradation mechanism.

Experimental setup

Photoreactors

The optimal conditions were evaluated by batch experiments using an open reactor ($V = 100$ mL) with an illuminated area (A1) of 471 cm^2, under magnetic stirring. A low-pressure

mercury vapor lamp (Our Lux 125 W) was used as the UVA radiation source. The pathway investigation and the scavenger participation on the IC dye photodegradation were carried out in a closed reactor, under magnetic stirring, with internal lighting, illuminated area (Ai) of 179 cm^2 and volume (V) of 500 mL. A low-pressure mercury vapor lamp (Philips TL 6 W) was used as UVA radiation source. The total incident radiant electromagnetic energy ($\lambda = 365$ nm) on the solution surface was measured using a portable radiometer 9811 Cole-Parmer Instrument Co. The average values determined were 2.64 mW cm^{-2} and 7.7 mW cm^{-2}, for the open and closed reactor, respectively.

Experimental design and procedure

A 2-level full factorial experimental design with 3 factors (k = 3) was made. The matrix of experiments was assembled using the factors: (1) photocatalyst (TiO_2) load, (2) pH and (3) IC concentration. The levels minimum (− 1) and maximum (+ 1) values (Rodrigues and Iemma 2014) of each variable are described in Table 1. The runs at intermediate level (0) were used for statistical analysis of the experiment reproducibility. A total of 12 experiments (Table 2) were performed, including a blank test (control) in the absence of the photocatalyst. The evaluated variable response was the residual IC dye concentration after 2 h of photocatalysis (C) divided by the initial concentration (C_0), C/C_0. No degradation was observed after 2 h (data not shown).

The variability of the IC dye photodegradation (C/C_0) was calculated using the center points conditions (0,0,0) (Schwaab and Pinto 2007) from the design of experiments (DOE) (Tables 1, 2). The experimental mean value found for C/C_0 was 0.0673 with a variance of 0.00004 and a standard deviation of 0.0067. In order to calculate the mean value (μ_x) and the standard deviation (σ_x^2) of the population (Table A1), a 95% confidence interval with 2 degrees of freedom (DL = $n - 1$) was used on the t-Student (Equation A1) and Chi-square (Equation A2) tests. The variability of the experimental mean value and standard deviation was in accordance with in the 95% confidence interval (Table A1). That said, the low variation between 3 replicas at the same conditions indicates that the experiment is well replicated, and same results were found.

Table 1 Minimum, intermediate and maximum concentrations of the input variables

Variable	[TiO_2] (mg L^{-1})	pH	[IC] (mg L^{-1})
− 1	2	4	6
0	7	7	8
+ 1	12	10	10

Table 2 Factorial experiment design matrix

Experiment	[TiO_2]	pH	[IC]
Blank	–	0	0
1	+ 1	+ 1	+ 1
2	− 1	+ 1	+ 1
3	+ 1	− 1	+ 1
4	− 1	− 1	+ 1
5	+ 1	+ 1	− 1
6	− 1	+ 1	− 1
7	+ 1	− 1	− 1
8	− 1	− 1	− 1
9	0	0	0
10	0	0	0
11	0	0	0

A fresh solution of IC was prepared for each experiment, in the proper concentration and pH, as described in Tables 1 and 2. Later, the IC solution was transferred into the reactor in continuous stirring, followed by the addition of TiO_2. The resulting suspension was kept in the dark for 30 min ($t = -30$ min), in order to reach adsorption equilibrium. Once the adsorption equilibrium is achieved, the observed decrease in concentration is associated with the degradation process instead (Satyro et al. 2014). The lamp was turned on after the dark step ($t = 0$). During the photocatalysis, samples were collected at different times ($t = -30$, 0, 15, 30, 45, 60, 90 and 120 min) for kinetics evaluation. At each sampling time, 5 mL of sample was taken using 10-mL syringe and filtered (nylon filters, $\phi_{filter} = 13$ mm, $\phi_{pore} = 0.20$ µm, Analytica) before analysis. Control samples were submitted to identical treatment. The experiments were performed twice, and mean values are presented.

It has been demonstrated little interference during the TiO_2/UV photocatalysis of dyes caused by average temperatures for wastewater treatment (Zhang et al. 2001; Zulmajdi et al. 2020). That said, all the experiments were conducted at room temperature ($T = 22 \pm 2$ °C).

The participation of the reactive species generated during photoexcitation of the semiconductor to the IC degradation was evaluated to determine the pathways and maximize the efficiency of IC degradation. Several scavengers (Table 3) were used during the photocatalysis.

The scavenger concentrations must be able to inhibit the reactive species generated in the TiO_2/UV process, and they were based on previously reported values (Jiménez et al. 2015; Bosio et al. 2018). Sodium azide (NaN_3) was employed as oxygen singlet ($^1O_2$) scavenger. Aliphatic alcohols (ROH) are used as radical hydroxyl scavenger. Iodide ions (I^-) are electron donors species and were used to inhibit the positive hole (h^+). Tert-butanol (t-BuOH) was added to inhibit hydroxyl radicals and to prevent the iodide oxidation to I_2/I_3^- (Rodríguez et al. 2014). To prevent photocatalytic

Table 3 Scavengers, concentrations and their roles in the investigation of IC photocatalytic degradation

	Scavenger 1 [M]	Scavenger 2 [M]	Reactive species inhibited
1	KI 0.01 1.3×10^{-4} 6.5×10^{-5}	–	Positive hole (h^+)
2	Na_3N 0.01 1.3×10^{-4} 6.5×10^{-5}	–	Singlet oxygen ($^1O_2$)
3	2-PrOH 0.1 1.3×10^{-4} 6.5×10^{-5}	–	Hydroxyl radical ($^{\cdot}OH$)
4	t-BuOH 0.1 1.3×10^{-4} 6.5×10^{-5}	–	Hydroxyl radical ($^{\cdot}OH$)
5	KI 0.01 1.3×10^{-4} 6.5×10^{-5}	t-BuOH 0.1 1.3×10^{-4} 6.5×10^{-5}	Positive hole (h^+) and hydroxyl radical ($^{\cdot}OH$)
6	Na_3N 1.3×10^{-4} 6.5×10^{-5}	t-BuOH 1.3×10^{-4} 6.5×10^{-5}	Singlet oxygen ($^1O_2$) and hydroxyl radical ($^{\cdot}OH$)

degradation through different paths at the same time, different scavengers were used at once to inhibit different mechanisms to happen. Optimal conditions were used on these experiments (Table 3), pH = 4.0, [IC] = 6 mg L^{-1} and [TiO_2] = 12 mg L^{-1}.

Analytical determinations

Indigo Carmine (IC) degradation was determined using a UV–Vis spectrophotometer (Thermo Scientific, model Multiskan). The breakage of the chromophore group (decolorization) was monitored at $\lambda = 610$ nm and the aromatic rings reduction at UV region (200–400 nm).

Total organic carbon (TOC) and total nitrogen (TN) were measured using a TOC Shimadzu equipment (TOC-V_{CPN} and TNM-1e) in order to determinate the mineralization level of the dye. The presence of anions, such as NO_3^-, NO_2^- and SO_4^{2-}, was determined by ion chromatography using a DIONEX ICS-90 equipment coupled to AS14 column and equipped with a conductivity detector, and a solution of Na_2CO_3 (0.002 M) and $NaHCO_3$ (0.01 M) was used as eluent. Ammonia ions (NH_4^+) present in solution were determined by Nessler method, in which 0.1 mL of Nessler reagent (potassium tetraiodomercurate (II) alkaline solution) was added to 5 mL of sample. This reaction forms $Hg_2O(NH_2)I^-$, a yellow compound that adsorbs at $\lambda = 425$ nm; later, its concentration is converted to ammonia concentration (APHA 2012). Thermal analyses (TG-DTG) of TiO_2 samples before and after IC photodegradation were carried out using a STA7300 HITACHI Thermal Analyzer from 273 to 1273 K under nitrogen flow (80 cm^3 min^{-1}).

Results and discussion

Optimum conditions for photocatalytic IC degradation

The blank experiment (control) performed in the absence of the photocatalyst at [IC] = 8 mg L^{-1} and pH 7.0 showed no IC dye degradation (data not shown) even after 2 h of irradiation exposure. This confirmed that IC is not photolyzed by UV light.

The kinetic of photocatalytic decolorization for most organic compounds is described by the pseudo-first-order kinetic model (Bentouami et al. 2010) (Eq. 1).

$$\frac{-dC}{dt} = k_{app}C \tag{1}$$

in which k_{app} (min^{-1}) is the apparent rate constant.

In this case, the relation between concentration found at time t (C_t) and the initial concentration (C_0) can be calculated by integrating Eq. 1, considering the limit condition $C_t = C_0$ at $t = 0$ (Eq. 2).

$$\ln\left(\frac{C_0}{C_t}\right) = k_{app}t \tag{2}$$

The k_{app} of each experiment was then estimated by plotting ln C_t versus reaction time t. At extreme tested pH conditions, pH = 10 and pH = 4 (Fig. 1 and Table 4), the kinetic data fit the pseudo-first order. The correlation coefficient values are higher than 0.984 for different pH values (Table 4).

The photocatalytic degradation at $[TiO_2] = 2$ mg L^{-1} had the lowest kinetic rates (Fig. 1b, d), which indicates that the pH had a minor effect on IC dye photodegradation. At $[TiO_2] = 2$ mg L^{-1} and [IC] = 10 mg L^{-1}, the kinetic rates were 0.192×10^{-2} and 0.133×10^{-2} min^{-1} at pH 10 and 4, respectively (Fig. 1b). At $[TiO_2] = 2$ mg L^{-1} and [IC] = 6 mg L^{-1}, the kinetic rates were 0.424×10^{-2} and 0.454×10^{-2} min^{-1}, at pH 10 and 4, respectively (Fig. 1d). The kinetic rates in both cases (Fig. 1d) are the lowest. This is mainly related to the lower concentration of photocatalyst, once the efficiency of degradation is related to the availability of active sites on the TiO_2 surface and on the ability of these sites to be reached by the light (Saggioro et al. 2015a).

Figure 1a, c shows the results at a higher load of TiO_2 (12 mg L^{-1}); as a result, higher kinetic degradation rates were achieved (Table 4). However, factors like pH (4 and 10) and [IC] (6 and 10 mg L^{-1}) demonstrated to also impact these rates. A decrease in the availability of oxidation sites on the photocatalyst surface might happen when larger amounts of the organic compound, IC dye, are adsorbed onto this surface, therefore affecting the degradation rate (Ajmal et al. 2016). It is possible to observe a trend, even if slightly, when varying the pH or the photocatalyst load (Fig. 1a, b), while at a higher concentration of IC dye (10 mg L^{-1}), which indicates that higher degradation rates are achieved at basic conditions (pH = 10).

The constants rates at $[TiO_2] = 12$ mg L^{-1} were 3.52×10^{-2} and 1.85×10^{-2} min^{-1} and at $[TiO_2] = 2$ mg L^{-1} were 0.192×10^{-2} and 0.133×10^{-2} min^{-1}, for basic (pH = 10) and acid conditions (pH = 4), respectively. This might be explained by the fact that the aromatic group in the dye molecule is unstable when in alkali conditions (Figure S1), causing loss of the hydrogen bound to the nitrogen, which makes it more susceptible to attack (Vautier et al. 2001; Saggioro et al. 2015a).

Greater degradation rates were found in acidic conditions (pH = 4) at a lower IC dye concentration (6 mg L^{-1}) (Fig. 1c). The constant rates at $[TiO_2] = 12$ mg L^{-1} were 2.00×10^{-2} and 5.22×10^{-2} min^{-1}, for basic (pH = 10) and acid conditions (pH = 4), respectively. In this case, the aromatic ring instability by the alkali condition (pH = 10) might not be enough to lead to IC degradation. The photocatalytic reaction occurs on the surface of photocatalyst, and it is dependent on the TiO_2 surface charge, meaning that the adsorptive properties of TiO_2 particles strongly depend on the pH of the solution (Ajmal et al. 2014). In this case, the repulsion between the sulfonic group present on the IC dye molecule and the negatively charged titanium dioxide surface (TiO^-) at pH = 10 ($TiO_{2pzc} = 6.8$) could have blocked the dye adsorption and, consequently, reducing the photocatalytic degradation rates. At pH = 4, the photocatalyst surface becomes positively charged, favoring the absorption process, and the opposite is then observed, according to Eqs. 3 and 4.

$$pH < pzc = TiOH + H^+ \leftrightarrow TiOH_2^+ \quad (3)$$

$$pH > pzc = TiOH + OH^- \leftrightarrow TiO^- + H_2O \quad (4)$$

Nitrate and sulfate were monitored during IC degradation (Fig. 2). The ratio between the nitrate concentrations at $t = 2$ h (C) and at $t = 0$ (C_0), C/C_0, was close to 1 for all the experiments. That said, there was no increase in nitrate concentrations after 2 h of photocatalytic degradation. Conversely, sulfate concentrations at $t = 4$ h were higher than the sulfate concentrations at $t = 0$ h ($C/C_0 > 1$) for all the experiments. This was a predominant effect observed on experiment 7 ($C/C_0 = 2.3$), which had the highest kinetic constant rate (5.22×10^{-2} min^{-1}). The structure of the IC dye is characterized by a chromophore group, carbon-to-carbon double bonds (–C=C–) that are usually attached to two-electron groups donors (NH) and receptors (CO) (maximum peak located at 610 nm) (Wahab and Hadi 2017). Besides that, IC dye has two sulfonic groups attached to two aromatic rings (absorbance peak at 287 nm) (Bentouami et al. 2010). The sulfate analysis after the IC dye degradation (Fig. 2) indicates that the release of sulfur ions in the solution, which probably originates from these sulfonic groups (Vautier et al. 2001). In addition, the sulfonic groups are responsible for the IC dye adsorption on the photocatalyst surface (Vautier et al. 2001). Therefore, it should be easier to remove the sulfur ions and release them in solution during photocatalysis than the nitrogen ions found on the molecule ring. In conclusion, there is an indication (Figs. 1c and 3; experiment 7—pH 4.0, [IC] = 6 mg L^{-1} and $[TiO_2] = 12$ mg L^{-1}) that the degradation occurred on carbon-to-carbon double bonds, causing the breakage and decolorization, and as well as on the sulfonic groups.

Finally, as experiment 7 (pH = 4.0, [IC] = 6 mg L^{-1} and $[TiO_2] = 12$ mg L^{-1}) was the instance with the higher kinetic constant rate (5.22×10^{-2} min^{-1} and $t_{1/2} = 13.25$ min) during the IC dye photocatalytic degradation, its conditions were used for further studies, such as the photodegradation mechanisms using different radicals and hole scavengers.

Photocatalytic mechanism of scavenger participation

Several reactive species, such as superoxide anion radicals ($O_2^{\cdot-}$), $^{\cdot}OH$ radicals and photogenerated holes (h^+), are able to degrade organic compounds (Benalioua et al. 2015; Jiménez et al. 2015). A strategy with different scavengers was

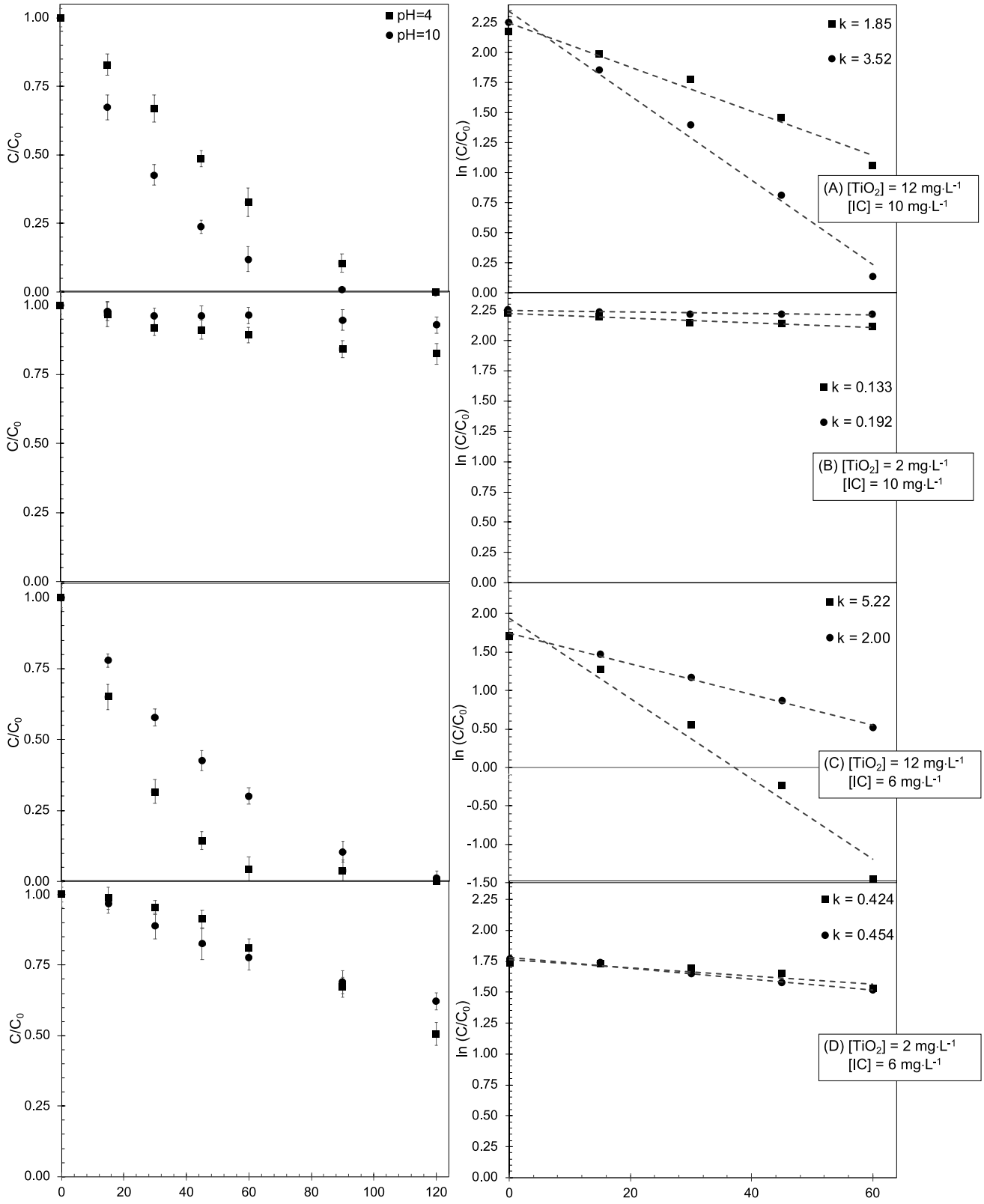

Fig. 1 pH Influence on IC photodegradation and respective pseudo-first-order rate constants (10^{-2} min^{-1})

Table 4 Kinetics constants and half-life time of IC for the photocatalytic experiments and their correlation coefficients

Experiment	k_{app} (min^{-1})	$t_{1/2}$ (min)	R^2
1	$3.52\times10^{-2}\pm0.029$	19.6875 ± 1.48	0.994 ± 0.001
2	$0.133\times10^{-2}\pm3.5\times10^{-5}$	521.0526 ± 13.89	0.998 ± 0.002
3	$1.85\times10^{-2}\pm0.0011$	37.4594 ± 2.30	0.987 ± 0.005
4	$0.192\times10^{-2}\pm4.72\times10^{-5}$	360.0937 ± 8.46	0.998 ± 0.001
5	$2.00\times10^{-2}\pm0.007$	34.65 ± 7.13	0.998 ± 0.001
6	$0.424\times10^{-2}\pm8.73\times10^{-5}$	163.4433 ± 3.24	0.999 ± 0.0005
7	$5.23\times10^{-2}\pm0.002$	13.2504 ± 0.49	0.984 ± 0.003
8	$0.454\times10^{-2}\pm6.65\times10^{-5}$	152.6431 ± 2.17	0.985 ± 0.004

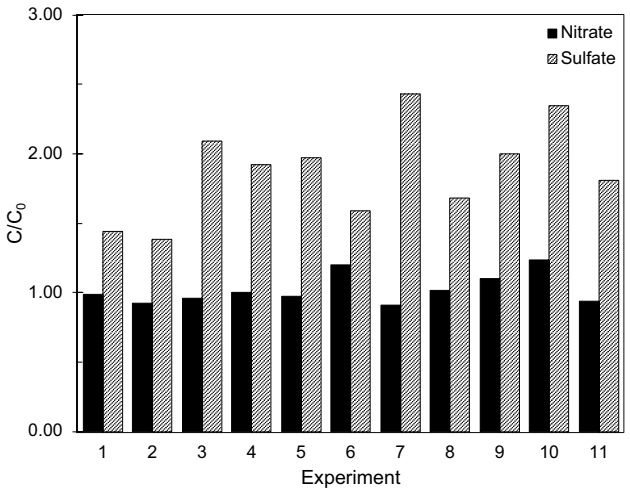

Fig. 2 Nitrate and sulfate concentrations after 2 h of photocatalytic degradation. $[TiO_2]=12$ mg L^{-1}, $[IC]=6$ mg L^{-1} and pH = 4

employed to investigate the photocatalytic mechanism and to evaluate the participation of the main reactive species involved in the IC dye degradation (Table 3). The effect of the scavengers concentration was also evaluated (Fig. 3). Higher scavenger concentrations did not inhibit IC photodegradation (Fig. 3a), which might be affected by other factors such as increasing dye adsorption onto the photocatalyst surface caused by high Na^+ or K^+ concentrations favoring photodegradation (Guasch et al. 2010). Nevertheless, experiments carried out at $[scavenger]=1.3\times10^{-4}$ M (Fig. 3b) and 6.5×10^{-5} M (Fig. 3c) inhibited IC photodegradation. The addition of KI (h^+ scavenger) decreases IC photodegradation in 30 min down to 52%, while in the absence of this scavenger IC photodegradation achieved 72%. At the same time, about 34% of degradation was inhibited in the presence of Na_3N (singlet oxygen scavenger). On the other hand, no effect was observed in the presence of any hydroxyl scavenger, such as t-BuOH and 2-PrOH. In their presence, IC photodegradation achieved 70 and 77% (t = 30 min), respectively. A minor participation of $^{\cdot}OH$ on IC photodegradation was observed when it was used combinations of scavengers, such as (1) $h^+ + {}^{\cdot}OH$ scavenger (KI + t-BuOH), and (2)

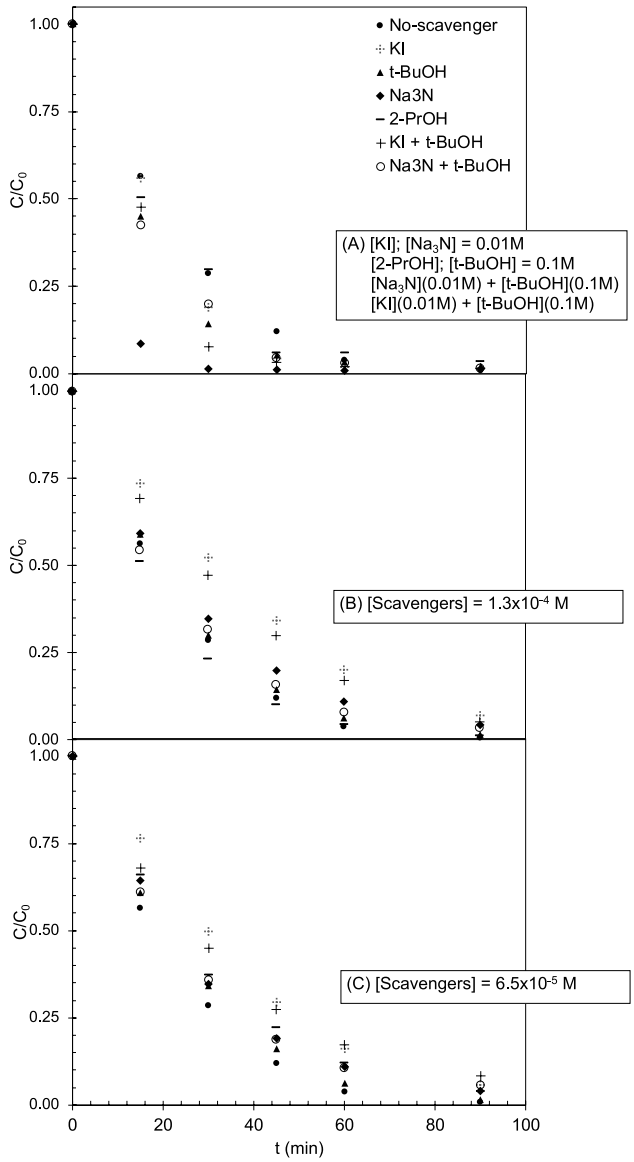

Fig. 3 Photocatalytic degradation as a function of irradiation time in the presence of different scavengers

singlet oxygen + $^{\cdot}OH$ scavenger (t-BuOH + Na_3N). These combinations resulted in lowering the IC photodegradation rates down to 47 and 31%, respectively, which are similar results than those achieved when h^+ *or* singlet oxygen alone was used.

The iodide ion (I^-) is oxidized (I_2/I_3^-) by hydroxyl radicals, ergo its concentration decreases, and so does its capacity as a hole scavenger (Rodríguez et al. 2014). In order to prevent that from happening, iodide anion was used also in the presence of t-BuOH, which acts as a hydroxyl radical scavenger (Rodríguez et al. 2014). This result indicates that h^+ is the major active species responsible for the IC photodegradation (Eqs. 5–6) followed by $O_2^{\cdot-}$ (Eqs. 5, 7–10) and $^{\cdot}OH$ (5, 11–14) under moderate and minor contribution, respectively:

$$TiO_2 + hv \rightarrow h^+_{VB} + e^-_{CB} \quad (5)$$

$$TiO_2\left(h^+\right) + \text{indigo carmine} \rightarrow TiO_2 + \text{transformation products} \quad (6)$$

$$dye + hv \rightarrow dye^* \quad (7)$$

$$dye^* + TiO_2 \rightarrow dye^{+\cdot} + TiO_2\left(e^-_{CB}\right) \quad (8)$$

$$TiO_2\left(e^-_{CB}\right) + O_2 \rightarrow TiO_2 + O_2^{\cdot-} \quad (9)$$

$$O_2^{\cdot-} + \text{indigo carmine} \rightarrow TiO_2 + \text{transformation products} \quad (10)$$

$$TiO_2\left(h^+\right) + H_2O \rightarrow TiO_2 + OH^{\cdot} + H^+ \quad (11)$$

$$TiO_2\left(h^+\right) + OH^- \rightarrow TiO_2 + OH^{\cdot} \quad (12)$$

$$TiO_2\left(e^-_{CB}\right) + H_2O_2 \rightarrow TiO_2 + OH^- + OH^{\cdot} \quad (13)$$

$$OH^{\cdot} + \text{indigo carmine} \rightarrow TiO_2 + \text{transformation products} \quad (14)$$

The findings on this study are in line with what was reported when two other catalysts were tested, Bi–Zn co-doped TiO_2/UV (Benalioua et al. 2015) and by Ag_2SO_4-deposited ZnO (Choo et al. 2016). It was reported that h^+ is the first responsible for the IC photodegradation. Interestingly enough, even if Benalioua et al. (2015) used a different catalyst, they also observed the same trend as this study did for the heterogenous photodegradation of IC dye ($h^+ > O_2^{\cdot-} > {}^{\cdot}OH$). The IC sulfonic groups play an important role on its absorption onto the photocatalyst surface due to their anionic characteristics. IC molecules could then be adsorbed onto the TiO_2 surface by a positive charge, providing the direct reaction with the positive hole (h^+) (Benalioua et al. 2015). This would be followed by action of the superoxide radical, as the second important active radical. Irradiation can photosensitize IC dye molecules to an excited single state (dye^*), which can potentially inject electrons on the TiO_2 conduction band (CB). This electron can react with oxygen molecules forming superoxide radical anions, $O_2^{\cdot-}$ (Choo et al. 2016). This degradation path is closely linked to the presence of oxygen; hence, intense stirring would be required to allow O_2 diffusion onto the semiconducting surface of the photocatalyst (Hernández-Gordillo et al. 2016).

Hydroxyl radicals are generated by adsorbed water molecules on the surface of photocatalyst. If IC molecules or its photo-by-products adsorb in the photocatalyst surface, the production of hydroxyl radicals will be reduced. Thermal analyses (TG-DTG) of TiO_2 before and after the photocatalysis were performed (Fig. 4). It was observed a total mass loss of 3 and 5% at lower temperatures (300–473 K) before and after being used in the photocatalysis, respectively. This is attributed to the loss of free adsorbed water onto the TiO_2 surface by hydrogen bonding (Gandhi et al. 2011). Furthermore, a second mass loss of approximately 2% in the range of 480–594 K was also observed, which could be related to compounds that remain adsorbed to the photocatalyst surface during IC photodegradation. This could interfere on the hydroxyl radical production and explain the minor participation of this radical on the IC degradation.

Mineralization assessment

Some indicators on the efficiency of photocatalytic treatments, such as total organic carbon (TOC) and total nitrogen (TN), are very useful since they reflect the achieved mineralization of the studied compounds. In this study, it was found no difference on the TOC and TN before and after photodegradation (Figure S2), indicating no or minor mineralization under the studied conditions. Therefore, IC was only converted to less complex organic molecules and an additional step would still be necessary to observe complete mineralization.

Chemical analyses indicate the presence of ammonia before the photocatalytic degradation (Figure S3), which is probably due to the presence of the IC dye synthesis residues since its purity grade is 85%. No increase was detected in the ammonia concentrations after the photocatalysis process in all experiments (Figure S3(b) and S3(c)) in the presence of the organic scavengers (t-BuOH and 2-PrOH) at lower concentrations. On the other hand, interferences were observed on the Nessler assay for the samples in which these organic scavengers (alcohols) were used at high concentrations (Figure S3a) (Guasch et al. 2010). No increase was observed in ammonia concentrations after the photocatalytic degradation indicates that

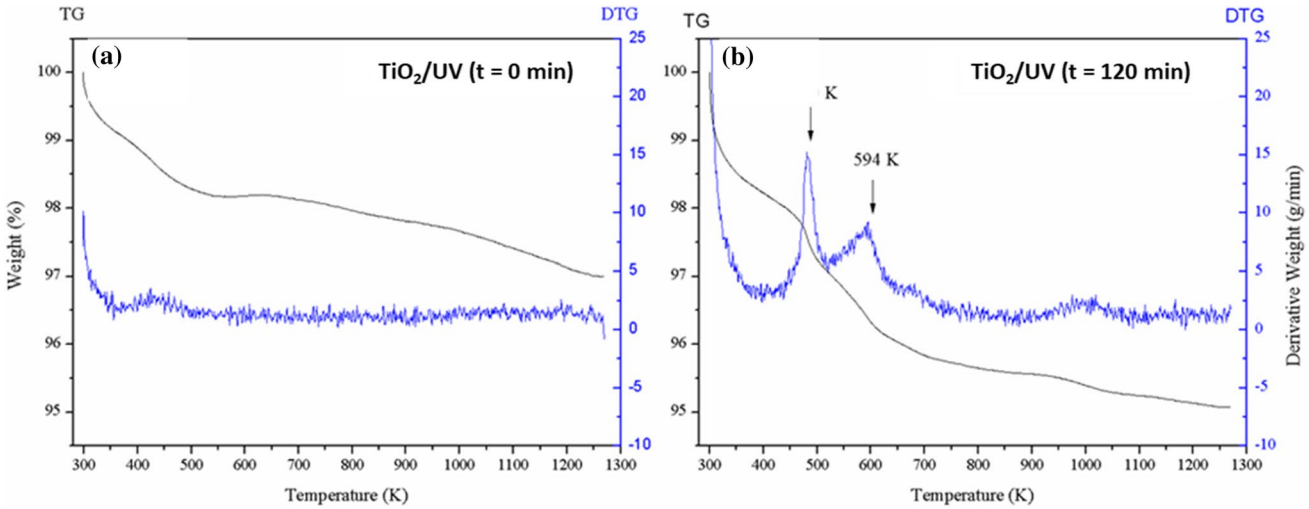

Fig. 4 TG-DTG profile of TiO_2 **a** 0 min and **b** after 120 min of the photocatalytic process

the nitrogen in the IC molecule is not released to the solution. Therefore, no rupture of the ring containing nitrogen occurred.

Conclusion

The mechanism and the kinetic of Indigo Carmine photodegradation using TiO_2 as the photocatalyst were investigated. The highest pseudo-first-order kinetics ($k = 5.22 \times 10^{-2}$ and $t_{1/2} = 13.25$ min) was achieved at pH = 4.0, [IC] = 6 mg L^{-1} and [TiO_2] = 12 mg L^{-1}. Photocatalytic degradation occurred via decolorization breaking the carbon-to-carbon double bonds and the aromatic rings. However, IC is not photolyzed and/or mineralized under the studied conditions. Thus, future studies should be carried out in order to achieve mineralization.

The results also suggest that IC degradation occurs, mainly, via oxidation of the positive hole (h^+) on the photocatalyst surface, followed by less impacting participations of superoxide anion and hydroxyl radical. According to the TG-DTG profile of TiO_2, the minor participation of hydroxyl radical can be attributed to compounds that remain adsorbed onto the photocatalyst surface during IC degradation. This minor participation results in no mineralization of the IC dye, since hydroxyl radicals are the main reactive species with higher oxidant potential that act on the carbon mineralization.

Acknowledgements The authors would like to thank the Brazilian National Research Council (CNPq) (Process n. 201488/2016-7) and Brazilian Coordination for the Improvement of Higher Education Personnel (CAPES) (Process n. 131639/2017-0) for financial support.

References

Ajmal A, Majeed I, Malik RN et al (2014) Principles and mechanisms of photocatalytic dye degradation on TiO_2 based photocatalysts: a comparative overview. RSC Adv 4:37003–37026

Ajmal A, Majeed I, Malik RN et al (2016) Photocatalytic degradation of textile dyes on Cu_2O–CuO/TiO_2 anatase powders. J Environ Chem Eng 4:2138–2146. https://doi.org/10.1016/j.jece.2016.03.041

APHA (2012) Standard methods for the examination of water and wastewater, 22nd edn. American Public Health Association, American Water Works Association, Water Environment Federation, Washington

Benalioua B, Mansour M, Bentouami A et al (2015) The layered double hydroxide route to Bi–Zn co-doped TiO_2 with high photocatalytic activity under visible light. J Hazard Mater 288:158–167. https://doi.org/10.1016/j.jhazmat.2015.02.013

Bentouami A, Ouali MS, De Menorval LC (2010) Photocatalytic decolourization of indigo carmine on 1,10-phenanthrolinium intercalated bentonite under UV-B and solar irradiation. J Photochem Photobiol A Chem 212:101–106. https://doi.org/10.1016/j.jphotochem.2010.04.002

Bosio M, Satyro S, Bassin JP et al (2018) Removal of pharmaceutically active compounds from synthetic and real aqueous mixtures and simultaneous disinfection by supported TiO_2/UV-A, H_2O_2/UV-A, and TiO_2/H_2O_2/UV-A processes. Environ Sci Pollut Res. https://doi.org/10.1007/s11356-018-2108-x

Brillas E (2020) A review on the photoelectro-Fenton process as efficient electrochemical advanced oxidation for wastewater remediation. Treatment with UV light, sunlight, and coupling with conventional and other photo-assisted advanced technologies. Chemosphere 250:126198. https://doi.org/10.1016/j.chemosphere.2020.126198

Cerreta G, Roccamante MA, Plaza-Bolaños P et al (2020) Advanced treatment of urban wastewater by UV-C/free chlorine process: micro-pollutants removal and effect of UV-C radiation on trihalomethanes formation. Water Res. https://doi.org/10.1016/j.watres.2019.115220

Choo HS, Lam SM, Sin JC, Mohamed AR (2016) An efficient Ag_2SO_4-deposited ZnO in photocatalytic removal of indigo carmine and phenol under outdoor light irradiation. Desalin

Water Treat 57:14227–14240. https://doi.org/10.1080/19443994.2015.1067833

Chowdhury AP, Shambharkar BH (2018) BiOBr–Ag_8SnS_6 heterostructured nanocomposite photocatalysts: synthesis, characterization, and photocatalytic application. Asia-Pac J Chem Eng 13:1–10. https://doi.org/10.1002/apj.2182

Das RS, Warkhade SK, Kumar A, Wankhade AV (2019) Graphene oxide-based zirconium oxide nanocomposite for enhanced visible light-driven photocatalytic activity. Res Chem Intermed 45:1689–1705. https://doi.org/10.1007/s11164-018-3699-z

Gandhi VG, Mishra MK, Rao MS et al (2011) Comparative study on nano-crystalline titanium dioxide catalyzed photocatalytic degradation of aromatic carboxylic acids in aqueous medium. J Ind Eng Chem 17:331–339. https://doi.org/10.1016/j.jiec.2011.02.035

Guasch H, Serra A, Corcoll N et al (2010) Metal ecotoxicology in fluvial biofilms: potential influence of water scarcity, pp 41–53. https://doi.org/10.1007/698_2009_25

Hernández-Gordillo A, Rodríguez-González V, Oros-Ruiz S, Gómez R (2016) Photodegradation of Indigo Carmine dye by CdS nanostructures under blue-light irradiation emitted by LEDs. Catal Today 266:27–35. https://doi.org/10.1016/j.cattod.2015.09.001

Höfl C, Sigl G, Specht O et al (1997) Oxidative degradation of aox and cod by different advanced oxidation processes: a comparative study with two samples of a pharmaceutical wastewater. Water Sci Technol 35:257–264. https://doi.org/10.1016/S0273-1223(97)00033-4

Jiménez M, Ignacio Maldonado M, Rodríguez EM et al (2015) Supported TiO_2 solar photocatalysis at semi-pilot scale: degradation of pesticides found in citrus processing industry wastewater, reactivity and influence of photogenerated species. J Chem Technol Biotechnol 90:149–157. https://doi.org/10.1002/jctb.4299

Kumar RV, Barbosa MO, Ribeiro AR et al (2020) Advanced oxidation technologies combined with direct contact membrane distillation for treatment of secondary municipal waste water. Process Saf Environ Prot. https://doi.org/10.1016/j.psep.2020.03.008

Labhane PK, Sonawane SH, Sonawane GH et al (2018) Influence of Mg doping on ZnO nanoparticles decorated on graphene oxide (GO) crumpled paper like sheet and its high photo catalytic performance under sunlight. J Phys Chem Solids 114:71–82. https://doi.org/10.1016/j.jpcs.2017.11.017

Rand MC, Greenberg AE, Taras MJ (eds) (1974) Method 350.2—nitrogen, ammonia (colorimetric, titrimetric, potentiometric distillation procedure). In: Standard methods for the examination of water and wastewater, 14th edn. American Public Health Association, Washington, p 1193

Rodrigues MI, Iemma AF (2014) Experimental design and process optimization. CRC Press, Boca Raton

Rodríguez EM, Márquez G, Tena M et al (2014) Determination of main species involved in the first steps of TiO_2 photocatalytic degradation of organics with the use of scavengers: the case of ofloxacin. Appl Catal B Environ 178:44–53. https://doi.org/10.1016/j.apcatb.2014.11.002

Rodríguez-González V, Obregón S, Patrón-Soberano OA et al (2020) An approach to the photocatalytic mechanism in the TiO_2-nanomaterials microorganism interface for the control of infectious processes. Appl Catal B Environ 270:118853

Saggioro EM, Oliveira AS, Buss DF et al (2015a) Photo-decolorization and ecotoxicological effects of solar compound parabolic collector pilot plant and artificial light photocatalysis of indigo carmine dye. Dye Pigment 113:571–580. https://doi.org/10.1016/J.DYEPIG.2014.09.029

Saggioro EM, Oliveira AS, Pavesi T et al (2015b) Solar CPC pilot plant photocatalytic degradation of indigo carmine dye in waters and wastewaters using supported-TiO_2: influence of photodegradation parameters. Int J Photoenergy. https://doi.org/10.1155/2015/656153

Salehi K, Bahmani A, Shahmoradi B et al (2017) Response surface methodology (RSM) optimization approach for degradation of Direct Blue 71 dye using CuO–ZnO nanocomposite. Int J Environ Sci Technol 14:2067–2076. https://doi.org/10.1007/s13762-017-1308-0

Satyro S, Marotta R, Clarizia L et al (2014) Removal of EDDS and copper from waters by TiO_2 photocatalysis under simulated UV-solar conditions. Chem Eng J 251:257–268. https://doi.org/10.1016/j.cej.2014.04.066

Schwaab M, Pinto JC (2007) Análise de Dados Experimentais: I. Fundamentos de Estatística e Estimação de Parametros, E-papers, Rio de Janeiro

Sharma S, Mehta SK, Ibhadon AO, Kansal SK (2019) Fabrication of novel carbon quantum dots modified bismuth oxide (α-Bi_2O_3/C-dots): material properties and catalytic applications. J Colloid Interface Sci 533:227–237. https://doi.org/10.1016/j.jcis.2018.08.056

Silva IFB, Martins AR, Krambrock K et al (2020) Understanding photocatalytic activity and mechanism of nickel-modified niobium mesoporous nanomaterials. J Photochem Photobiol A Chem 388:112168. https://doi.org/10.1016/j.jphotochem.2019.112168

Vautier M, Guillard C, Herrmann JM (2001) Photocatalytic degradation of dyes in water: case study of indigo and of indigo carmine. J Catal 201:46–59. https://doi.org/10.1006/jcat.2001.3232

Wahab HS, Hadi HM (2017) Visible light N-TiO_2-induced photodegradation of congo red: characterization, kinetics and mechanistic study. Int J Environ Sci Technol 14:2135–2148. https://doi.org/10.1007/s13762-017-1361-8

Zhang T, Oyama T, Aoshima A et al (2001) Photooxidative N-demethylation of methylene blue in aqueous TiO_2 dispersions under UV irradiation. J Photochem Photobiol A Chem 140:163–172. https://doi.org/10.1016/S1010-6030(01)00398-7

Zulmajdi SLN, Zamri NII, Yasin HM et al (2020) Comparative study on the adsorption, kinetics, and thermodynamics of the photocatalytic degradation of six different synthetic dyes on TiO_2 nanoparticles. React Kinet Mech Catal 129:519–534. https://doi.org/10.1007/s11144-019-01701-x